

$\bar{B} \rightarrow X_s \gamma$ in two universal extra dimensionsAyres Freitas¹ and Ulrich Haisch²¹ *Department of Physics and Astronomy, University of Pittsburgh, PA 15260, USA
and Enrico Fermi Institute, University of Chicago, Chicago, IL 60637, USA
and HEP Division, Argonne National Laboratory, Argonne, IL 60439, USA*² *Institut für Physik (THEP), Johannes Gutenberg-Universität D-55099 Mainz, Germany
and Institut für Theoretische Physik, Universität Zürich, CH-8057 Zürich, Switzerland*

(Dated: November 3, 2021)

We calculate the leading order corrections to the $\bar{B} \rightarrow X_s \gamma$ decay in the standard model with two large flat universal extra dimensions. We find that the contributions involving the exchange of Kaluza-Klein modes of the physical scalar field $a_{(kl)}^{\pm}$ depend logarithmically on the ultraviolet cut-off scale Λ . We emphasize that all flavor-changing neutral current transitions suffer from this problem. Although the ultraviolet sensitivity weakens the lower bound on the inverse compactification radius $1/R$ that follows from $\bar{B} \rightarrow X_s \gamma$, the constraint remains stronger than any other available direct measurement. After performing a careful study of the potential impact of cut-off and higher-order effects, we find $1/R > 650$ GeV at 95% confidence level if errors are combined in quadrature. Our limit is at variance with the parameter region $1/R \lesssim 600$ GeV preferred by dark matter constraints.

PACS numbers: 12.15.Lk, 12.60.-i, 13.25.Hw

I. INTRODUCTION

The branching ratio of the inclusive radiative \bar{B} -meson decay is known to provide stringent constraints on various non-standard physics models at the electroweak scale [1], because it is accurately measured and its theoretical determination is rather precise.

The present experimental world average, which includes the latest measurements by CLEO [2], Belle [3], and BaBar [4], is performed by the Heavy Flavor Averaging Group [5] and reads for a photon energy cut of $E_\gamma > E_0$ with $E_0 = 1.6$ GeV in the \bar{B} -meson rest-frame¹

$$\mathcal{B}(\bar{B} \rightarrow X_s \gamma)_{\text{exp}} = (3.55 \pm 0.24_{-0.10}^{+0.09} \pm 0.03) \times 10^{-4}. \quad (1)$$

Here the first error is a combined statistical and systematic one, while the second and third are systematic uncertainties due to the extrapolation from $E_0 = (1.8 - 2.0)$ GeV to the reference value and the subtraction of the $\bar{B} \rightarrow X_d \gamma$ event fraction, respectively.

After a joint effort [7, 8, 9], the first theoretical estimate of the total $\bar{B} \rightarrow X_s \gamma$ branching ratio at next-to-next-to-leading order (NNLO) in QCD has been presented recently in Refs. [8, 10]. For $E_0 = 1.6$ GeV the result of the improved standard model (SM) evaluation is given by²

$$\mathcal{B}(\bar{B} \rightarrow X_s \gamma)_{\text{SM}} = (3.15 \pm 0.23) \times 10^{-4}, \quad (2)$$

where the uncertainties from hadronic power corrections ($\pm 5\%$), higher-order perturbative effects ($\pm 3\%$), the interpolation in the charm quark mass ($\pm 3\%$), and parametric dependences ($\pm 3\%$) have been added in quadrature to obtain the total error.

Compared with the experimental world average of Eq. (1), the new SM prediction of Eq. (2) is lower by 1.2σ . Potential beyond SM contributions should now be preferably constructive, while models that lead to a suppression of the $b \rightarrow s \gamma$ amplitude are more severely constrained than in the past, where the theoretical determination used to be above the experimental one.

As emphasized in Refs. [13, 14, 15], among the latter category is the model with a flat, compactified extra dimension where all of the SM fields are allowed to propagate in the bulk [16], known as minimal universal extra dimensions or UED5. Since Kaluza-Klein (KK) modes in the UED5 model interfere destructively with the SM $b \rightarrow s \gamma$ amplitude, the $\mathcal{B}(\bar{B} \rightarrow X_s \gamma)$ constraint leads to a very powerful bound on the inverse compactification radius of $1/R > 600$ GeV at 95% confidence level (CL) [15]. This exclusion is independent from the Higgs mass and therefore stronger than any limit that can be derived from electroweak precision measurements [17].

The purpose of this article is to study the phenomenology of $\bar{B} \rightarrow X_s \gamma$ in the SM with two universal extra dimensions [18, 19] or UED6. In contrast to UED5, the UED6 model has additional KK particles in its spectrum. An interesting feature of this model is the fact that dark matter constraints suggest a rather small KK mass scale. Therefore it is very interesting to derive a bound on this scale from $b \rightarrow s \gamma$ in UED6, taking into account the new KK modes. In this context, several questions will need to be answered: Does the leading order (LO) result depend on the cut-off scale, in contrast to UED5 where no cut-off dependence was found? If so, is this a generic feature of all flavor-changing neutral current (FCNC) amplitudes

¹ The very recent measurement of BaBar [6] that gives $\mathcal{B}(\bar{B} \rightarrow X_s \gamma) = (3.66 \pm 0.85_{\text{stat}} \pm 0.60_{\text{sys}}) \times 10^{-4}$ for $E_0 = 1.9$ GeV is not taken into account in the average of Eq. (1).

² The small NNLO corrections related to the four-loop $b \rightarrow sg$ mixing diagrams [9] and from quark mass effects to the electromagnetic dipole [11] and current-current operator [12] contributions are not included in Eq. (2).

in the UED6 model? What is the theoretical uncertainty stemming from the unknown ultraviolet (UV) dynamics?

This article is organized as follows. In Secs. II and III we describe, first, the model itself and, second, the calculation of the one-loop matching corrections to the Wilson coefficients of the electro- and chromomagnetic dipole operators in UED6. Sec. IV contains a numerical analysis of $\mathcal{B}(\bar{B} \rightarrow X_s \gamma)$ and the lower bound on the compactification scale $1/R$ in the UED6 model. Concluding remarks are given in Sec. V. In App. A we show how to compute the double sums over KK modes appearing in the calculation of $\bar{B} \rightarrow X_s \gamma$.

II. MODEL

Here we briefly summarize the main features of the UED6 scenario. All SM fields propagate in two flat extra dimensions, compactified on a square with side length $L = \pi R$ and adjacent sides being identified [20]. This compactification, aptly dubbed chiral square, leads to chiral fermion zero modes, while the higher KK modes of the fermions are vector-like as usual. Since the geometry is invariant under rotations by 180° about the center of the square, the model respects an additional Z_2 symmetry. It implies that the lightest KK-odd particle is stable and could provide a viable dark matter candidate for a small KK scale $1/R \lesssim 600$ GeV [21].

Solving the six-dimensional equations of motion leads to an orthonormal set of functions, which depend on two KK indices k, l corresponding to the two extra dimensions, with $k \geq 1, l \geq 0$ or $k = l = 0$ [18]. The model becomes strongly interacting at high energy scales, so that it is viewed as a low-energy effective theory which is valid up to some cut-off scale Λ . From naive dimensional analysis (NDA) [19], this scale is estimated to be $\Lambda \approx 10/R$, corresponding to an upper limit $N_{\text{KK}} \leq k + l \approx 10$ for the KK indices.

Before electroweak symmetry breaking, all (kl) modes have degenerate tree-level masses $m_{(kl)} = \sqrt{k^2 + l^2}/R$. The degeneracy is lifted by loop corrections, which lead to mass operators localized at the corners of the chiral square [19, 22]. Additional flavor diagonal and non-diagonal contributions can originate from physics at the UV cut-off scale. Since flavor non-universal operators would in general lead to unacceptably large FCNC transitions, we will assume that the localized operators are fla-

vor conserving, so that the Cabibbo-Kobayashi-Maskawa (CKM) matrix remains the only source of flavor violation. In this work, we concentrate on the leading order contributions from the UED6 model to $\bar{B} \rightarrow X_s \gamma$, using tree-level masses for those KK excitations which receive only logarithmic corrections from loop corrections and boundary terms localized at the orbifold fixed points [19, 22, 23, 24]. This is justified since these terms are of one-loop order, thus leading to next-to-leading order effects for $\bar{B} \rightarrow X_s \gamma$.

Upon compactification, the six-component gauge fields W_M^a , $M = 0, \dots, 5$, decompose into four-component massive KK vector bosons $W_{\mu(kl)}^a$, $\mu = 0, \dots, 3$, and two scalar KK fields $W_{4,5(kl)}^a$. Here a denotes the adjoint group index. Following Refs. [18, 25], a covariant gauge fixing is introduced, such that $W_{\mu(kl)}^a$ do not mix with $W_{4,5(kl)}^a$. In the six-dimensional formulation, the gauge fixing-term reads

$$\begin{aligned} \mathcal{L}_{\text{GF}} = & -\frac{1}{2\xi} \left[\partial^\mu W_\mu^a - \xi(\partial_4 W_4^a + \partial_5 W_5^a - g_6 v_6 \chi^a) \right]^2 \\ & -\frac{1}{2\xi'} \left[\partial^\mu B_\mu - \xi'(\partial_4 B_4 + \partial_5 B_5 + g'_6 v_6 \chi^3) \right]^2, \end{aligned} \quad (3)$$

where W, B are the uncompactified $SU(2)$ and $U(1)$ gauge fields with the six-dimensional gauge couplings $g_6^{(\prime)}$, and $\xi^{(\prime)}$ are the gauge parameters. The χ^a are the components of the six-dimensional Higgs doublet

$$H = \frac{1}{\sqrt{2}} \begin{pmatrix} \chi^2 + i\chi^1 \\ v_6 + h + i\chi^3 \end{pmatrix}. \quad (4)$$

The six-dimensional gauge couplings and vacuum expectation value are related to the four-dimensional values by $g_6^{(\prime)} = g^{(\prime)} \pi R$ and $v_6 = v/R$.

The Higgs scalars mix with the fourth and fifth component of the gauge fields to form the would-be Goldstone bosons $G_{(kl)}^a$ of the massive vector bosons $W_{\mu(kl)}^a$, and two physical scalars $a_{(kl)}^a$ and $W_{H(kl)}^a$. Only the would-be Goldstone bosons have zero modes $G_{(00)}^a$, which correspond to the usual components of the SM Higgs doublet. For $k + l \geq 1$, the $G_{(kl)}^a$ are dominated by the scalar adjoints $W_{4,5(kl)}^a$ and $B_{4,5(kl)}$ while the $a_{(kl)}^a$ are composed mostly of the Higgs doublet elements. For the charged fields one finds

$$\begin{aligned} G_{(kl)}^\pm &= \frac{1}{M_W^{(kl)}} \left[\frac{1}{R} \left(l W_{4(kl)}^\pm - k W_{5(kl)}^\pm \right) + M_W \chi_{(kl)}^\pm \right], \\ a_{(kl)}^\pm &= \frac{1}{M_W^{(kl)}} \left[m_{(kl)} \chi_{(kl)}^\pm - \frac{M_W}{m_{(kl)} R} \left(l W_{4(kl)}^\pm - k W_{5(kl)}^\pm \right) \right], \\ W_{H(kl)}^\pm &= \frac{1}{\sqrt{k^2 + l^2}} \left[k W_{4(kl)}^\pm + l W_{5(kl)}^\pm \right], \end{aligned} \quad (5)$$

where

$$X^\pm = \frac{X^1 \mp iX^2}{\sqrt{2}}, \quad X = W, \chi, G, a, W_H. \quad (6)$$

Here $M_{W^{(kl)}}^2 = m_{(kl)}^2 + M_W^2$ is the tree-level squared mass of the $W_{\mu,H^{(kl)}}^\pm$ and $a_{(kl)}^\pm$. The would-be Goldstone bosons $G_{(kl)}^\pm$ receive the unphysical squared mass $\xi M_{W^{(kl)}}^2$ from gauge fixing. Similar expressions hold for the neutral fields, taking into account a small mixing between $W_{(kl)}^3$ and $B_{(kl)}$. However, since they do not contribute to the process $\bar{B} \rightarrow X_s \gamma$ at leading order in the electroweak interactions we do not give them here.

As mentioned above, the masses of the KK modes receive corrections from loop and UV effects, which are dependent on the cut-off scale Λ . Since $G_{(kl)}^\pm$ and $W_{\mu,H^{(kl)}}^\pm$ are protected by gauge invariance, the dependence on Λ is only logarithmic [22], so that the mass corrections are small compared to $1/R$ and can be neglected in a LO calculation. The $a_{(kl)}^\pm$ scalars, however, can receive contributions proportional to Λ^2 to both their bulk and boundary mass terms [24].

In order to obtain a small mass term for the zero mode Higgs doublet, the bulk and boundary mass terms need to be tuned to cancel to a large extent. However, independent of this tuning, the higher KK modes can receive sizeable contributions from these terms. As a result, the $a_{(kl)}^\pm$ scalars can be heavier or lighter than the other particles of the same KK level.³ We include the Λ^2 corrections to the $a_{(kl)}^\pm$ masses based on the following parametrization of the UV-induced mass terms:

$$\mathcal{L} \supset \left[\frac{L^2}{2} (\delta(x_4)\delta(x_5) + \delta(L-x_4)\delta(L-x_5)) m_{H,1}^2 + \frac{L^2}{2} \delta(x_4)\delta(L-x_5) m_{H,2}^2 + m_{H,\text{bulk}}^2 \right] |H|^2. \quad (7)$$

Although the UV physics is not specified, these mass parameters are expected to stem from loop contributions of the UV dynamics, so that

$$m_{H,i}^2 = \frac{h_i^2}{16\pi^2} \Lambda^2 = \frac{h_i^2}{16\pi^2} \frac{N_{\text{KK}}^2}{R^2}, \quad i = 1, 2, \quad (8)$$

with $h_{1,2} = \mathcal{O}(1)$. Using the explicit form of the KK wave functions from Refs. [18, 20] and tuning the bulk mass $m_{H,\text{bulk}}^2$ to exactly cancel the Λ^2 correction to the zero mode of the Higgs doublet, the masses of the $a_{(kl)}^\pm$ scalars are found to be

$$M_{a^{(kl)}}^2 = M_{W^{(kl)}}^2 + \frac{3h_1^2 + (1 + (-2)^{k+l})h_2^2}{16\pi^2} \frac{N_{\text{KK}}^2}{R^2}. \quad (9)$$

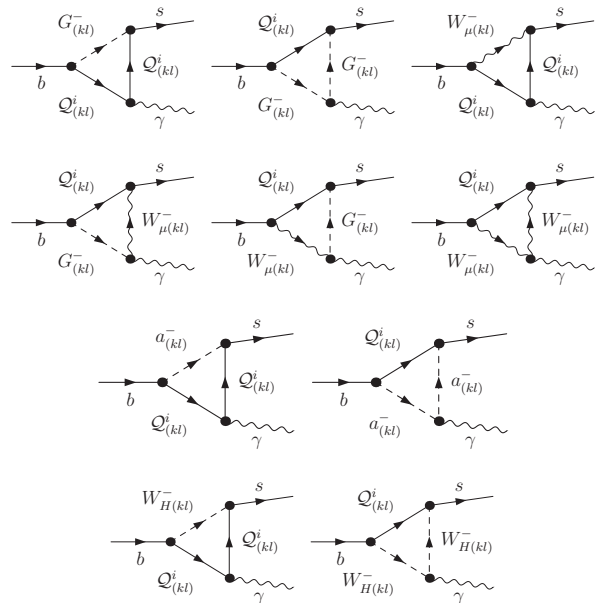


FIG. 1: One-loop corrections to the $b \rightarrow s \gamma$ amplitude in the UED6 model involving the KK modes of the would-be Goldstone, $G_{(kl)}^\pm$, the W -boson, $W_{\mu^{(kl)}}^\pm$, and the scalar fields $a_{(kl)}^\pm$ and $W_{H^{(kl)}}^\pm$. Diagrams where the $SU(2)$ quark doublets $Q_{(kl)}^i$ are replaced by the $SU(2)$ quark singlets $U_{(kl)}^i$ are not shown. Here $i = u, c, t$. See text for details.

We will estimate the theoretical uncertainty from the unspecified UV physics by varying the coupling constants $h_{1,2}$ of the boundary mass terms independently in the range $[0, 1]$ which corresponds to either decoupling or strong coupling.

The boundary mass terms could cause mixing among KK modes and one would need to re-diagonalize the mass matrix to find the eigenstates if they are large. To have a light Higgs boson, we assume that these mixing mass terms are tuned to be much smaller than $1/R$, so that we can treat them as small perturbations and ignore the higher-order mixing effects.

The small KK scale suggested by dark matter constraints would lead to interesting signals at the Fermilab Tevatron and the CERN Large Hadron Collider [19, 26, 27] as well as the International Linear Collider [28]. However, strong bounds on the compactification radius can arise from heavy flavor physics. In particular, the FCNC decay $\bar{B} \rightarrow X_s \gamma$, which shall be studied in the following, is known to put stringent constraints on various beyond the SM physics scenarios at the electroweak scale.

III. CALCULATION

We work in an effective theory with five active quarks, photons and gluons obtained by integrating out the electroweak bosons, the top quark, and all the heavy KK

³ This problem already arises in UED5, but was not discussed in previous analyses of $\bar{B} \rightarrow X_s \gamma$ for this model [13, 14, 15].

modes. Adopting the operator basis of Ref. [29], the effective Lagrangian relevant for the $b \rightarrow s\gamma(g)$ transitions at a scale μ reads

$$\mathcal{L}_{\text{eff}} = \mathcal{L}_{\text{QED} \times \text{QCD}} + \frac{4G_F}{\sqrt{2}} V_{ts}^* V_{tb} \sum_{i=1}^8 C_i(\mu) Q_i, \quad (10)$$

where the first term is the conventional QED and QCD Lagrangian for the light SM particles. In the second term G_F and V_{ij} denotes the Fermi coupling constant and the elements of the CKM matrix, respectively, while $C_i(\mu)$ are the Wilson coefficients of the corresponding operators Q_i build out of the light fields. Terms proportional to the small V_{ub} mixing, which will be included in our numerical results, have been neglected above for simplicity. The same refers to higher-order electroweak corrections [30].

The operators $Q_{1,\dots,6}$ are the usual four-quark operators whose explicit form can be found in Ref. [29]. The remaining two operators, characteristic for the $b \rightarrow s\gamma(g)$ transitions, are the dipole operators

$$\begin{aligned} Q_7 &= \frac{em_b}{16\pi^2} (\bar{s}_L \sigma^{\mu\nu} b_R) F_{\mu\nu}, \\ Q_8 &= \frac{gm_b}{16\pi^2} (\bar{s}_L \sigma^{\mu\nu} T^a b_R) G_{\mu\nu}^a. \end{aligned} \quad (11)$$

Here $e(g)$ is the electromagnetic (strong) coupling constant, $q_{L,R}$ are chiral quark fields, $F_{\mu\nu}$ ($G_{\mu\nu}^a$) is the electromagnetic (gluonic) field strength tensor, and T^a are the color generators normalized such that $\text{Tr}(T^a T^b) = \delta_{ab}/2$. The factor \overline{m}_b in the definition of $Q_{7,8}$ denotes the bottom quark $\overline{\text{MS}}$ mass renormalized at μ .

The relevant quantity entering the calculation of $\mathcal{B}(\overline{B} \rightarrow X_s \gamma)$ is not $C_7(\mu)$ but a linear combination $C_7^{\text{eff}}(\mu)$ of this Wilson coefficient and of the coefficients of the four-quark operators. The so-called effective Wilson coefficients relevant for $b \rightarrow s\gamma(g)$ are [31]

$$C_i^{\text{eff}}(\mu) = \begin{cases} C_i(\mu) & \text{for } i = 1, \dots, 6, \\ C_7(\mu) + \sum_{j=1}^6 y_j C_j(\mu) & \text{for } i = 7, \\ C_8(\mu) + \sum_{j=1}^6 z_j C_j(\mu) & \text{for } i = 8, \end{cases} \quad (12)$$

where y_j and z_j are chosen so that the LO $b \rightarrow s\gamma(g)$ matrix elements of the effective Lagrangian are proportional to the LO terms $C_{7,8}^{\text{eff}(0)}(\mu)$. In the $\overline{\text{MS}}$ scheme with fully anticommuting γ_5 , one has $\vec{y} = (0, 0, -\frac{1}{3}, -\frac{4}{9}, -\frac{20}{3}, -\frac{80}{9})$ and $\vec{z} = (0, 0, 1, -\frac{1}{6}, 20, -\frac{10}{3})$ [29].

We further decompose the effective coefficients into a SM and a new physics part

$$C_i^{\text{eff}}(\mu) = C_{i\text{SM}}^{\text{eff}}(\mu) + \Delta C_i^{\text{eff}}(\mu), \quad i = 1, \dots, 8, \quad (13)$$

and expand the latter contribution in powers of α_s as follows

$$\Delta C_i^{\text{eff}}(\mu) = \sum_{n=0}^{\infty} \left(\frac{\alpha_s(\mu)}{4\pi} \right)^n \Delta C_i^{\text{eff}(n)}(\mu). \quad (14)$$

In the case of UED6, new physics affects the initial conditions of the Wilson coefficients of the operators in the low-energy effective theory while it does not induce new operators besides those already present in the SM. To find the LO corrections from the UED6 model to $\mathcal{B}(\overline{B} \rightarrow X_s \gamma)$ one has to consider all the one-loop one-particle-irreducible diagrams contributing to the processes $b \rightarrow s\gamma(g)$. The one-loop $b \rightarrow s\gamma$ diagrams are shown in Fig. 1. Before performing the loop integration, the Feynman integrands are Taylor-expanded up to second order in the off-shell external momenta and to first order in the bottom quark mass. Thereby only terms which project on Q_7 after the use of the equations of motion are retained. The calculation for the $b \rightarrow sg$ amplitude proceeds in the same way. The relevant Feynman rules have been derived from Ref. [18] and implemented into a model file for **FeynArts 3** [32], which has been used to generate the necessary amplitudes. At tree-level, the interactions between SM and KK fields preserve both KK numbers. Consequently, only diagrams where all particles in the loop have the same KK index (kl) have to be taken into account.

At the matching scale $\mu_0 = \mathcal{O}(m_t)$ the LO results for the UED6 initial conditions read

$$\Delta C_i^{\text{eff}(0)}(\mu_0) = \begin{cases} 0 & \text{for } i = 1, \dots, 6, \\ -\frac{1}{2} \sum'_{k,l} A^{(0)}(x_{kl}) & \text{for } i = 7, \\ -\frac{1}{2} \sum'_{k,l} F^{(0)}(x_{kl}) & \text{for } i = 8, \end{cases} \quad (15)$$

where the \prime superscript in the summation indicates that the KK sums run only over the restricted range $k \geq 1$ and $l \geq 0$, *i.e.* $\sum'_{k,l} = \sum_{k \geq 1} \sum_{l \geq 0}$.

We decompose the Inami-Lim functions as

$$X^{(0)}(x_{kl}) = \sum_{I=W,a,H} X_I^{(0)}(x_{kl}), \quad X = A, F, \quad (16)$$

where the function $X_{W,a,H}^{(0)}(x_{kl})$ describes the contribution due to the exchange of KK modes of the would-be Goldstone, $G_{(kl)}^\pm$, and the W -bosons, $W_{\mu(kl)}^\pm$, the scalar fields $a_{(kl)}^\pm$ and $W_{H(kl)}^\pm$. Here $x_{kl} = (k^2 + l^2)/(R^2 M_W^2)$.

Our results for the LO Inami-Lim functions entering Eq. (16) are given by

$$A_W^{(0)}(x_{kl}) = \frac{x_t (6((x_t - 3)x_t + 3)x_{kl}^2 - 3(5(x_t - 3)x_t + 6)x_{kl} + x_t(8x_t + 5) - 7)}{12(x_t - 1)^3} + \frac{1}{2}(x_{kl} - 2)x_{kl}^2 \ln\left(\frac{x_{kl}}{x_{kl} + 1}\right) - \frac{(x_{kl} + x_t)^2(x_{kl} + 3x_t - 2)}{2(x_t - 1)^4} \ln\left(\frac{x_{kl} + x_t}{x_{kl} + 1}\right), \quad (17)$$

$$F_W^{(0)}(x_{kl}) = \frac{x_t (-6((x_t - 3)x_t + 3)x_{kl}^2 - 3((x_t - 3)x_t + 6)x_{kl} + (x_t - 5)x_t - 2)}{4(x_t - 1)^3} - \frac{3}{2}(x_{kl} + 1)x_{kl}^2 \ln\left(\frac{x_{kl}}{x_{kl} + 1}\right) + \frac{3(x_{kl} + 1)(x_{kl} + x_t)^2}{2(x_t - 1)^4} \ln\left(\frac{x_{kl} + x_t}{x_{kl} + 1}\right), \quad (18)$$

$$A_a^{(0)}(x_{kl}) = \frac{x_t (6x_{kl}^2 - 3(x_t(2x_t - 9) + 3)x_{kl} + (29 - 7x_t)x_t - 16)}{36(x_t - 1)^3} - \frac{1}{6}(x_{kl} - 2)x_{kl} \ln\left(\frac{x_{kl}}{x_{kl} + 1}\right) - \frac{(x_{kl} + 3x_t - 2)(x_t + x_{kl}((x_{kl} - x_t + 4)x_t - 1))}{6(x_t - 1)^4} \ln\left(\frac{x_{kl} + x_t}{x_{kl} + 1}\right), \quad (19)$$

$$F_a^{(0)}(x_{kl}) = \frac{x_t (-6x_{kl}^2 + (6x_t^2 - 9x_t - 9)x_{kl} + (7 - 2x_t)x_t - 11)}{12(x_t - 1)^3} + \frac{1}{2}x_{kl}(x_{kl} + 1) \ln\left(\frac{x_{kl}}{x_{kl} + 1}\right) + \frac{(x_{kl} + 1)(x_t + x_{kl}((x_{kl} - x_t + 4)x_t - 1))}{2(x_t - 1)^4} \ln\left(\frac{x_{kl} + x_t}{x_{kl} + 1}\right), \quad (20)$$

$$A_H^{(0)}(x_{kl}) = \frac{x_t (6(x_t^2 - 3x_t + 3)x_{kl}^2 - 3(3x_t^2 - 9x_t + 2)x_{kl} - 7x_t^2 + 29x_t - 16)}{36(x_t - 1)^3} + \frac{1}{6}x_{kl}(x_{kl}^2 - x_{kl} - 2) \ln\left(\frac{x_{kl}}{x_{kl} + 1}\right) - \frac{(x_{kl} + 1)(x_{kl}^2 + (4x_t - 2)x_{kl} + x_t(3x_t - 2))}{6(x_t - 1)^4} \ln\left(\frac{x_{kl} + x_t}{x_{kl} + 1}\right), \quad (21)$$

$$F_H^{(0)}(x_{kl}) = -\frac{x_t (6(x_t^2 - 3x_t + 3)x_{kl}^2 + 3(3x_t^2 - 9x_t + 10)x_{kl} + 2x_t^2 - 7x_t + 11)}{12(x_t - 1)^3} - \frac{1}{2}x_{kl}(x_{kl} + 1)^2 \ln\left(\frac{x_{kl}}{x_{kl} + 1}\right) + \frac{(x_{kl} + x_t)(x_{kl} + 1)^2}{2(x_t - 1)^4} \ln\left(\frac{x_{kl} + x_t}{x_{kl} + 1}\right). \quad (22)$$

Here $x_t = m_t^2(\mu_0)/M_W^2$. Our results for the sums $X_W^{(0)}(x_{kl}) + X_a^{(0)}(x_{kl})$, $X = A, F$, agree with the expressions for the one-loop dipole functions given in Ref. [14]. We note that there is a misprint in the last line of Eq. (3.33) of the latter paper. Obviously, the term $\ln((x_n + x_t)/(1 + x_t))$ should read $\ln((x_n + x_t)/(1 + x_n))$ with $x_n = n^2/(R^2 M_W^2)$ and n the single KK index appearing in UED5.

For the numerical analysis, the results in Eqs. (17) to (22) need to be summed over the KK indices k, l . This summation can be performed analytically employing an expansion for large $1/R$, as explained in App. A. For zero boundary mass contributions, $h_{1,2} = 0$, we obtain the following approximate formulas

$$\sum_{k,l}' A_W^{(0)}(x_{kl}) \approx \frac{0.686134 + 0.162912 \Delta x_t}{x^2}, \quad (23)$$

$$\sum_{k,l}' F_W^{(0)}(x_{kl}) \approx \frac{0.316677 + 0.075190 \Delta x_t}{x^2}, \quad (24)$$

$$\sum_{k,l}' A_a^{(0)}(x_{kl}) \approx -\frac{23\pi x_t}{288 x} \ln(\Lambda^2 R^2) - \frac{0.86695 + 0.205844 \Delta x_t}{x}, \quad (25)$$

$$\sum_{k,l}' F_a^{(0)}(x_{kl}) \approx -\frac{7\pi x_t}{96 x} \ln(\Lambda^2 R^2) - \frac{0.791563 + 0.187945 \Delta x_t}{x}, \quad (26)$$

$$\sum_{k,l}' A_H^{(0)}(x_{kl}) \approx -\frac{0.211118 + 0.050127 \Delta x_t}{x^2}, \quad (27)$$

$$\sum_{k,l}' F_H^{(0)}(x_{kl}) \approx -\frac{0.158339 + 0.037595 \Delta x_t}{x^2}, \quad (28)$$

where $x = 1/(R^2 M_W^2)$ and $\Delta x_t = x_t - (165/80.4)^2$. Note that in the above formulas we have only kept the leading terms in the $1/x$ expansion for simplicity. The coefficients of the logarithms in Eqs. (25) and (26) are exact in the limit of an infinite number of KK modes. We em-

phasize that the given approximations are for illustrative purpose only. In our numerical analysis we will throughout employ the exact double series $\sum_{k,l} X_I^{(0)}(x_{kl})$, $X = A, F, I = W, a, H$, summed over the restricted range $k \geq 1$, $l \geq 0$, and $l + k \leq N_{\text{KK}}$.

We see from the latter equations that while the one-loop $G_{(kl)}^\pm$ and $W_{\mu,H(kl)}^\pm$ corrections to $\Delta C_{7,8}^{\text{eff}(0)}(\mu_0)$ are insensitive to the UV cut-off scale Λ or, equivalently, N_{KK} , the contributions due to $a_{(kl)}^\pm$ exchange depend logarithmically on Λ . The different convergence behavior is closely connected to the unitarity of the CKM matrix which results in a Glashow-Iliopoulos-Maiani (GIM) suppression [33] of the higher KK mode contributions to the double sums in Eqs. (23) to (28). In the case at hand, the GIM mechanism leads to a hierarchy of the various contributions to $\Delta C_{7,8}^{\text{eff}(0)}(\mu_0)$, with $X_{W,H}^{(0)}(x_{kl})$ proportional to $1/(k^2 + l^2)^2$ and $X_a^{(0)}(x_{kl})$, $X = A, F$, scaling like $1/(k^2 + l^2)$ for large values of l, k . The extra power of $k^2 + l^2$ in the contribution from diagrams with $a_{(kl)}^\pm$ exchange, that leads to the logarithmic divergent results, stems from the left- (right-handed) top quark Yukawa coupling enhanced part of the $a_{(kl)}^+ \bar{U}_{(kl)}^t b$ ($a_{(kl)}^- \bar{s} U_{(kl)}^t$) tree-level vertex. No such terms are present in the flavor-changing vertices involving $G_{(kl)}^\pm$ and $W_{\mu,H(kl)}^\pm$.

The logarithmic divergences appearing in Eqs. (25) and (26) would be cancelled by counterterms at the scale Λ at which perturbativity is lost in the higher dimensional theory. Our calculation only determines the leading logarithmic corrections associated with the renormalization group (RG) running between Λ and $1/R$. The corresponding initial conditions contain incalculable finite matching corrections from the unknown UV physics. Assuming that the RG effects dominate over the finite matching corrections and that the UV completion of the UED6 model has a CKM-type flavor structure, the UV sensitivity can be absorbed into a logarithmic dependence on ΛR or, equivalently, N_{KK} . To gauge the theoretical uncertainty associated with the unknown UV completion we will vary N_{KK} in the range [5, 15] around $N_{\text{KK}} = \Lambda R \approx 10$ as estimated by NDA. The choice of the lower value of N_{KK} is motivated by the observation that for $N_{\text{KK}} < 5$ the non-logarithmic terms in $\sum_{k,l} X_a^{(0)}(x_{kl})$, $X = A, F$, become numerically of the same size as the logarithmic ones. Since the choice of the upper value of N_{KK} has no impact on our conclusions we choose it symmetrically. We mention that the requirement of unitarity of gauge boson scattering at high energies [34] generically leads to values of ΛR notably below the NDA estimate $N_{\text{KK}} \approx 10$.

The individual contributions $\Delta_I C_{7,8}^{\text{eff}(0)}(\mu_0)$, $I = W, a, H$, to the UED6 initial conditions of the dipole operators as a function of $1/R$ are shown in Fig. 2. The contribution due to the exchange of $G_{(kl)}^\pm$ and $W_{\mu(kl)}^\pm$ and $W_{H(kl)}^\pm$ (green/medium gray) KK modes are depicted as yellow (light gray) and green (medium gray) curves, while the red (dark gray) bands and the black

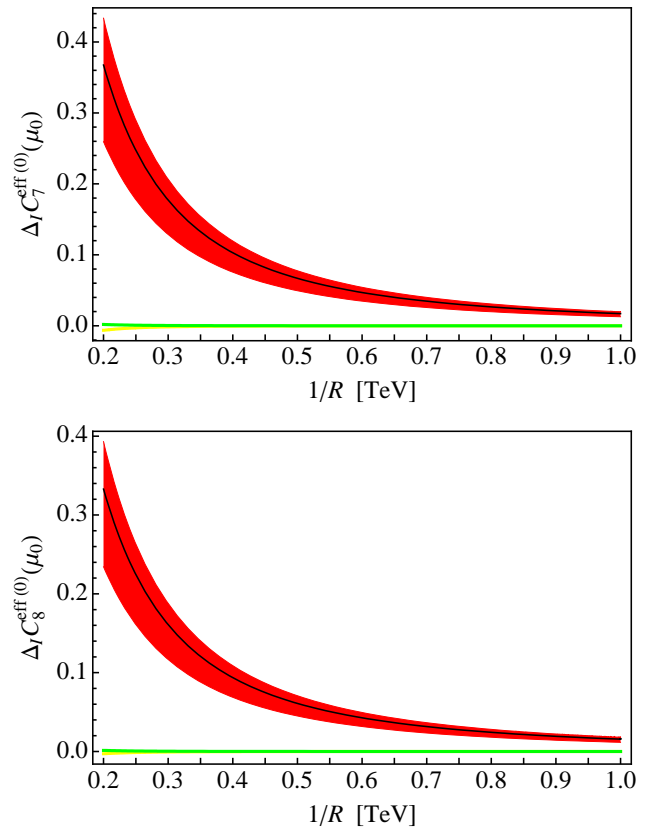


FIG. 2: $\Delta_I C_{7,8}^{\text{eff}(0)}(\mu_0)$ as a function of $1/R$. The different curves correspond to the individual contributions due to the exchange of KK modes of the would-be Goldstone, $G_{(kl)}^\pm$, and the W -bosons, $W_{\mu(kl)}^\pm$ (yellow/light gray), the scalar fields $a_{(kl)}^\pm$ (black) and $W_{H(kl)}^\pm$ (green/medium gray), respectively. The lower (upper) borders of the red (dark gray) bands correspond to $N_{\text{KK}} = 5$ (15) while the black lines represent the results for $N_{\text{KK}} = 10$. See text for details.

lines illustrate the $a_{(kl)}^\pm$ corrections. The lower (upper) borders of the red (dark gray) bands correspond to $N_{\text{KK}} = 5$ (15) while the black lines represent the results for $N_{\text{KK}} = 10$. We see that in both cases the contribution involving $a_{(kl)}^\pm$ exchange is by far dominant and its variation with N_{KK} is non-negligible. Nevertheless, the large positive corrections to $\Delta C_{7,8}^{\text{eff}(0)}(\mu_0)$ already start to exceed the SM values $C_{7,8}^{\text{eff}(0)}(\mu_0) \approx -0.19, -0.10$ in magnitude for $1/R \approx 240, 335$ GeV in the most conservative case $N_{\text{KK}} = 5$. The observed strong enhancement of the initial conditions $C_{7,8}^{\text{eff}(0)}(\mu_0)$ will play the key role in our phenomenological applications.⁴

⁴ For compactification scales $1/R \approx 100$ GeV it would even be possible to reverse the sign of $C_7^{\text{eff}}(\mu_b)$ with respect to its SM value $C_7^{\text{eff}}(\mu_b) \approx -0.37$. This possibility is disfavored on general grounds by the experimental information on $\bar{B} \rightarrow X_s l^+ l^-$ [35].

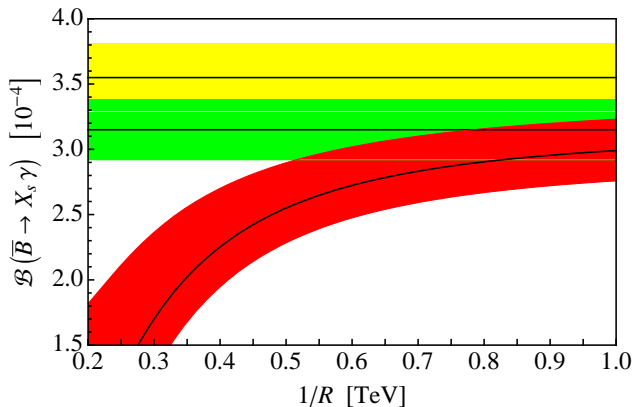


FIG. 3: $\mathcal{B}(\bar{B} \rightarrow X_s \gamma)$ for $E_0 = 1.6$ GeV as a function of $1/R$. The red (dark gray) band corresponds to the UED6 result. The 68% CL range and central value of the experimental/SM result is indicated by the yellow/green (light/medium gray) band underlying the straight solid line. See text for details.

Another main observation of our work is, that in the UED6 model the Z - (ΔC), photon (ΔD), gluon penguin (ΔE), and the $|\Delta F| = 2$ boxes (ΔS) all behave as $1/(k^2 + l^2)$ for large values of k, l . In contrast, $|\Delta F| = 1$ boxes ($\Delta B_{\nu\nu, ll}$) show an asymptotic $1/(k^2 + l^2)^2$ behavior after GIM. The corresponding UED6 Inami-Lim functions therefore exhibit the following behavior: $\Delta C, \Delta S \propto x_t^2/x \ln(\Lambda^2 R^2)$, $\Delta D, \Delta E \propto x_t/x \ln(\Lambda^2 R^2)$, and $\Delta B_{\nu\nu, ll} \propto x_t/x^2$. This implies that the logarithmic cut-off sensitivity first seen in Eqs. (25) and (26) is a generic feature of all FCNC transitions in the UED6 model. A dedicated study of neutral meson mixing, rare K - and B -decays in UED6 is left for further work.

IV. NUMERICS

The UED6 prediction of $\mathcal{B}(\bar{B} \rightarrow X_s \gamma)$ for $E_0 = 1.6$ GeV as a function of $1/R$ is displayed by the red (dark gray) band in Fig. 3. The yellow (light gray) and green (medium gray) band in the same figure shows the experimental and SM result as given in Eqs. (1) and (2), respectively. In all three cases, the middle line is the central value, while the widths of the bands indicate the uncertainties that one obtains by adding errors in quadrature. The central value of the UED6 prediction corresponds to $N_{\text{KK}} = 10$ and $h_{1,2} = 0$. The strong suppression of $\mathcal{B}(\bar{B} \rightarrow X_s \gamma)$ in the UED6 model with respect to the SM expectation and the slow decoupling of KK modes is clearly seen in Fig. 3.

In our numerical analysis, matching of the UED6 Wilson coefficients at the electroweak scale is complete up to leading logarithmic order, while terms beyond that order include SM contributions only. For the reference values of the renormalization scales $\mu_0, \mu_b, \mu_c = 160, 2.5, 1.25$ GeV,

we utilize the formula

$$\begin{aligned} \mathcal{B}(\bar{B} \rightarrow X_s \gamma) = & \left[3.15 \pm 0.23 \right. \\ & - 8.03 \Delta C_7^{\text{eff}(0)}(\mu_0) - 1.92 \Delta C_8^{\text{eff}(0)}(\mu_0) \\ & + 4.96 (\Delta C_7^{\text{eff}(0)}(\mu_0))^2 + 0.36 (\Delta C_8^{\text{eff}(0)}(\mu_0))^2 \\ & \left. + 2.33 \Delta C_7^{\text{eff}(0)}(\mu_0) \Delta C_8^{\text{eff}(0)}(\mu_0) \right] \times 10^{-4}, \end{aligned} \quad (29)$$

which has been derived based on the NNLO SM results of Refs. [8, 10, 36]. For the remaining input parameters we adopt the central values and error ranges that can be found in Ref. [8].

The theoretical uncertainty in the UED6 model is estimated by scanning N_{KK} , the couplings $h_{1,2}$ of the boundary mass terms, and the matching scale μ_0 in the range [5, 15], [0, 1], and [80, 320] GeV for the largest possible variations. The combined theory error does not exceed $^{+17}_{-8}\%$ for $1/R$ in the range [0.4, 2.0] TeV. Larger relative errors of above $^{+55}_{-25}\%$ appear for $1/R = 300$ GeV. Whether the quoted numbers provide a reliable estimate of the cut-off and higher-order corrections to $\mathcal{B}(\bar{B} \rightarrow X_s \gamma)$ in the UED6 model can only be seen by performing a next-to-leading order (NLO) matching calculation. Such a calculation seems worthwhile but is beyond the scope of this work. The parametric uncertainty due to the error on the top quark mass is below $^{+1}_{-3}\%$ for $1/R$ in the range [0.3, 2.0] TeV and thus notably smaller than the combined theory uncertainty.

Since the experimental result is at present above the SM one and KK modes in the UED6 model necessarily interfere destructively with the SM $b \rightarrow s \gamma$ amplitude, the lower bound on $1/R$ following from $\mathcal{B}(\bar{B} \rightarrow X_s \gamma)$ turns out to be much stronger than what one can derive from any other currently available direct measurement [26]. If experimental, parametric, and theory uncertainties are treated as Gaussian and combined in quadrature, the 95% CL bound amounts to 650 GeV. In contrast to the upper limit coming from the dark matter abundance the latter exclusion is almost independent of the Higgs mass because genuine electroweak effects related to Higgs boson exchange enter $\mathcal{B}(\bar{B} \rightarrow X_s \gamma)$ first at the two-loop level. In the SM these corrections have been calculated [30] and amount to around -1.5% in the branching ratio. They are included in Eq. (29). Neglecting the corresponding two-loop Higgs effects in the UED6 model calculation should therefore have practically no influence on the derived limits.

The upper (lower) contour plot in Fig. 4 shows the 95% CL bound of $1/R$ as a function of the experimental (SM) central value and error. The current experimental world average and SM prediction of Eqs. (1) and (2) are indicated by the black squares. These plots allow to monitor the effect of future improvements in both the measurements and the SM prediction. Of course, one should keep in mind that the derived bounds depend in a non-negligible way on the treatment of theoretical uncertainties. Furthermore, the found limits could be weakened by

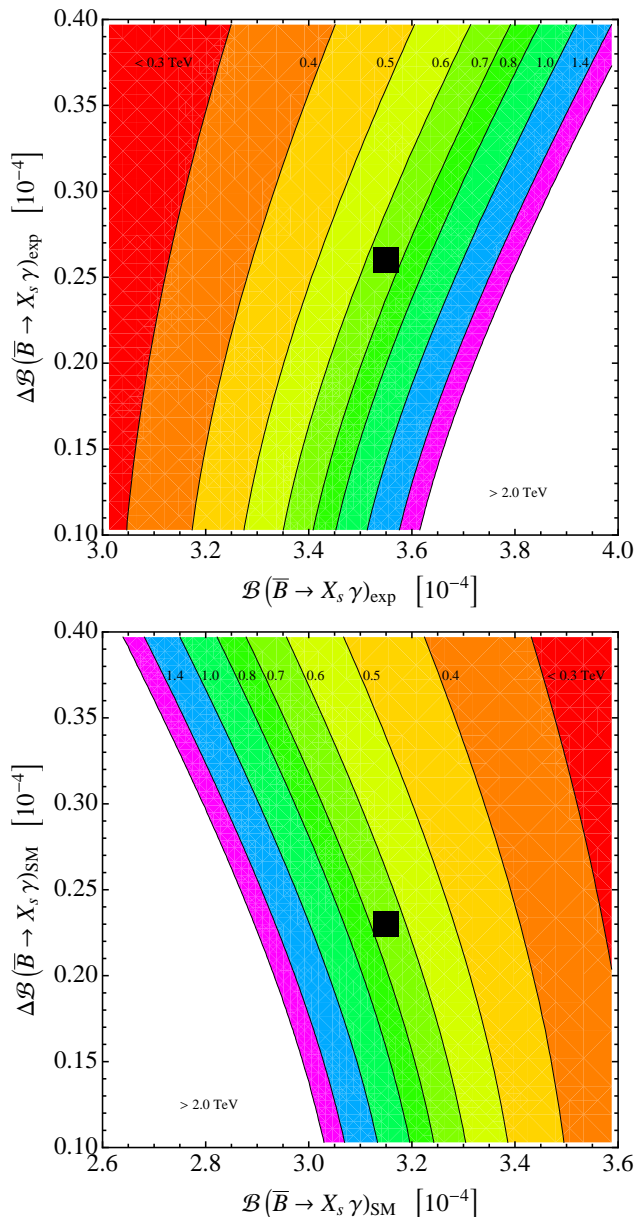


FIG. 4: The upper/lower panel displays the 95% CL limits on $1/R$ as a function of the experimental/SM central value (horizontal axis) and total error (vertical axis). The experimental/SM result from Eq. (1)/Eq. (2) is indicated by the black square. The contour lines represent values that lead to the same bound in TeV. See text for details.

APPENDIX A: EVALUATION OF KK SUMS

Here we show how to approximate the double sum over KK levels (kl) appearing in Eq. (15). Following Ref. [25], we first introduce the integrals

$$I_n(a) = (-1)^n a^{n+1} \int_0^1 dy \frac{y^n}{ay + x_{kl}}, \quad (\text{A1})$$

the NLO matching corrections in the UED6 model which remain unknown.

V. CONCLUSIONS

We have calculate the leading order corrections to the inclusive radiative $\bar{B} \rightarrow X_s \gamma$ decay in the standard model with two universal extra dimensions. While the one-loop matching corrections associated to the exchange of Kaluza-Klein modes of the would-be Goldstone, $G_{(kl)}^\pm$, the W -boson, $W_{\mu(kl)}^\pm$, and the physical scalar $W_{H(kl)}^\pm$ are insensitive to the ultraviolet physics, we find that contributions involving $a_{(kl)}^\pm$ scalars depend logarithmically on the cut-off scale Λ . We have emphasized that in the considered model all flavor-changing neutral current transitions suffer from this problem already at leading order. Moreover, we have included formally next-to-leading, but sizeable mass corrections to the Kaluza-Klein scalars that depend quadratically on the scale Λ . Although the ultraviolet sensitivity weakens the lower bound on the inverse compactification radius $1/R$ that can be derived from the measurements of the $\bar{B} \rightarrow X_s \gamma$ branching ratio, a strong constraint of $1/R > 650$ GeV at 95% confidence level is found if errors are added in quadrature. Our bound exceeds by far the limits that can be derived from any other direct measurement, and is at variance with the parameter region preferred by the dark matter abundance. This once again underscores the outstanding role of the inclusive radiative \bar{B} -meson decay in searches for new physics close to the electroweak scale.

Acknowledgments

We are grateful to Mikolaj Misiak and Matthias Steinhauser for private communications concerning Eq. (29). Helpful discussions with Bogdan Dobrescu and Giulia Zanderighi are acknowledged. ANL is supported by the U.S. Department of Energy, Division of High Energy Physics, under Contract DE-AC02-06CH11357. This work was initiated when U. H. was supported by the Swiss Nationalfonds. He is grateful to the University of Zürich for the pleasant working environment during that time.

where $n = 0, 1, \dots$, and $x_{kl} = (k^2 + l^2)x$ with $x = 1/(R^2 M_W^2)$. Obviously, $I_n(0) = 0$. These integrals allow us to express the logarithms appearing in Eqs. (17) to (22) as

$$\begin{aligned} \ln\left(\frac{x_{kl} + a}{x_{kl} + 1}\right) &= I_0(a) - I_0(1), \\ x_{kl} \ln\left(\frac{x_{kl} + a}{x_{kl} + 1}\right) &= I_1(a) - I_1(1) - 1 + a, \\ x_{kl}^2 \ln\left(\frac{x_{kl} + a}{x_{kl} + 1}\right) &= I_2(a) - I_2(1) + \frac{1}{2} - x_{kl} + x_{kl}a - \frac{1}{2}a^2, \\ x_{kl}^3 \ln\left(\frac{x_{kl} + a}{x_{kl} + 1}\right) &= I_3(a) - I_3(1) - \frac{1}{3} + \frac{1}{2}x_{kl} - x_{kl}^2 + x_{kl}^2a - \frac{1}{2}x_{kl}a^2 + \frac{1}{3}a^3, \end{aligned} \tag{A2}$$

with $a = 0$ or x_t . We note that Eq. (D.3) of Ref. [25] is missing an overall minus sign on its right-hand side.

Since the individual building blocks $I_n(a)$ behave as $1/(k^2 + l^2)$ for large k, l , the corresponding double series over the KK levels diverge logarithmically. We regulate the appearing divergence analytically

$$I_n^\delta(a) = (-1)^n a^{n+1} \int_0^1 dy \frac{y^n}{(ay + x_{kl})^{1+\delta}}, \tag{A3}$$

with $\delta > 0$. Then one has

$$\begin{aligned} \sum'_{k,l} I_n^\delta(a) &= (-1)^n a^{n+1} \sum_{k=1}^{\infty} \sum_{l=0}^{\infty} \int_0^1 dy \frac{y^n}{(ay + x_{kl})^{1+\delta}} \\ &= \frac{(-1)^n a^{n+1}}{\Gamma(1+\delta)} \sum_{k=1}^{\infty} \sum_{l=0}^{\infty} \int_0^1 dy y^n \int_0^{\infty} dt t^\delta e^{-(ay+x_{kl})t} \\ &= \frac{(-1)^n a^{n+1}}{4\Gamma(1+\delta)} \int_0^1 dy y^n \int_0^{\infty} dt t^\delta \left(\vartheta_3(0, e^{-xt})^2 - 1 \right) e^{-ayt} \\ &= \frac{(-1)^n}{4\Gamma(1+\delta)} \int_0^{\infty} dt t^{-1-n+\delta} \left(\vartheta_3(0, e^{-xt})^2 - 1 \right) (\Gamma(1+n) - \Gamma(1+n, at)), \end{aligned} \tag{A4}$$

where in the first step we have used the Mellin-Barnes representation

$$\frac{1}{s^{1+\delta}} = \frac{1}{\Gamma(1+\delta)} \int_0^{\infty} dt t^\delta e^{-st}. \tag{A5}$$

Here $\vartheta_3(u, q) = 1 + 2 \sum_{m=1}^{\infty} q^{m^2} \cos(2mu)$, $\Gamma(z) = \int_0^{\infty} dt t^{z-1} e^{-t}$ and $\Gamma(u, z) = \int_z^{\infty} dt t^{u-1} e^{-t}$, denotes the elliptic theta, the Euler gamma, and the plica function, respectively.

The integration over t in the last line of Eq. (A4) cannot be performed analytically. Yet using

$$\vartheta_3(0, e^{-z}) \approx \begin{cases} \sqrt{\frac{\pi}{z}}, & \text{for } z \leq \sqrt{\pi}, \\ 1 + 2 \sum_{m=1}^{n+1} e^{-m^2 z}, & \text{for } z > \sqrt{\pi}, \end{cases} \tag{A6}$$

and expanding the integrand in powers of $1/t$ in the latter case, we can perform the integration piecewise and approximate the double series as

$$\sum'_{k,l} I_n^\delta(a) \approx l_n^\delta(a) + h_n(a). \tag{A7}$$

The integration over $t \in [0, \sqrt{\pi}/x]$ leads to the relatively compact formulas

$$l_n^\delta(a) = \frac{(-1)^n \pi a^{n+1}}{4(n+1)x} \frac{1}{\delta} + \begin{cases} \frac{1}{8x} \left[2\sqrt{\pi} x E_2 \left(\frac{a\sqrt{\pi}}{x} \right) - x \left(2\Gamma \left(0, \frac{a\sqrt{\pi}}{x} \right) + \ln \left(\frac{a^2 \pi}{x^2} \right) \right) \right. \\ \left. + 2 \left(\pi a (1 - \ln a) - (\sqrt{\pi} + \gamma_E) x \right) \right], & \text{for } n = 0, \\ \frac{(-1)^n}{4n(n+1)^2 x} \left[e^{-\frac{a\sqrt{\pi}}{x}} (n+1)^2 x a^n - a^n \left(x(n+1)^2 \right. \right. \\ \left. \left. + \pi a n (n+1) \left(\Gamma \left(0, \frac{a\sqrt{\pi}}{x} \right) + \ln(a) \right) - \pi a n \right) \right. \\ \left. \left. + (n+1) (n(1 - \sqrt{\pi}) + 1) \pi^{-n/2} x^{n+1} \right. \right. \\ \left. \left. \times \left(\Gamma(n+1) - \Gamma \left(n+1, \frac{a\sqrt{\pi}}{x} \right) \right) \right] \right], & \text{for } n = 1, 2, \dots, \end{cases} \quad (\text{A8})$$

where we have expanded the result around $\delta = 0$ and dropped all terms that vanish in the limit $\delta \rightarrow 0$. Furthermore, $E_m(z) = \int_1^\infty dt t^{-m} e^{-zt}$ and $\gamma_E \approx 0.577216$ is the exponential integral function and the Euler constant.

The integration over $t \in (\sqrt{\pi}/x, \infty)$ is finite in the limit $\delta \rightarrow 0$. For all double sums $\sum'_{k,l} I_n(a)$ appearing in Eq. (A2) we were able to find analytic expressions. Since the results turn out to be rather lengthy and not very informative we refrain from giving them here. Short numerical expressions for the $h_n(a)$ can be obtained in the large x limit. Keeping terms up to third order in $1/x$, we find

$$h_n(a) = \begin{cases} \frac{0.184616 a}{x} - \frac{0.25221 a^2}{x^2} + \frac{0.259202 a^3}{x^3}, & \text{for } n = 0, \\ -\frac{0.0923082 a^2}{x} + \frac{0.16814 a^3}{x^2} - \frac{0.194402 a^4}{x^3}, & \text{for } n = 1, \\ \frac{0.0615388 a^3}{x} - \frac{0.126105 a^4}{x^2} + \frac{0.155522 a^5}{x^3}, & \text{for } n = 2, \\ -\frac{0.0461541 a^4}{x} + \frac{0.100884 a^5}{x^2} - \frac{0.129601 a^6}{x^3}, & \text{for } n = 3. \end{cases} \quad (\text{A9})$$

Combining Eqs. (A8) and (A9) we finally arrive at the following large x approximations

$$\sum'_{k,l} I_n^\delta(a) \approx \frac{(-1)^n \pi a^{n+1}}{4(n+1)x} \left(\frac{1}{\delta} - \ln x \right) + \begin{cases} \frac{0.644381 a}{x} - \frac{0.751902 a^2}{x^2} + \frac{0.387481 a^3}{x^3}, & \text{for } n = 0, \\ -\frac{0.322191 a^2}{x} + \frac{0.501268 a^3}{x^2} - \frac{0.290611 a^4}{x^3}, & \text{for } n = 1, \\ \frac{0.214794 a^3}{x} - \frac{0.375951 a^4}{x^2} + \frac{0.232489 a^5}{x^3}, & \text{for } n = 2, \\ -\frac{0.161095 a^4}{x} + \frac{0.300761 a^5}{x^2} - \frac{0.193741 a^6}{x^3}, & \text{for } n = 3. \end{cases} \quad (\text{A10})$$

The term $1/\delta - \ln x$ in Eq. (A10) implies that one should include counterterm contributions from physics at the UV cut-off scale Λ that cancel the divergences. Our calculation only determines the RG running contribution between Λ and $1/R$, given initial conditions at Λ . Assuming that the unknown finite matching corrections are small and have a CKM-type flavor structure, the divergences can be absorbed into a cut-off dependence by switching from analytic to cut-off regularization employing the approximation

$$\frac{1}{\delta} - \ln x \approx \ln(\Lambda^2 R^2), \quad (\text{A11})$$

with Λ not much larger than $1/R$. We remark that the latter assumptions are self-consistent because the finite matching corrections are formally of next-to-leading logarithmic order.

-
- [1] For a recent review see U. Haisch, 0706.2056 [hep-ph].
- [2] S. Chen *et al.* [CLEO Collaboration], Phys. Rev. Lett. **87** (2001) 251807.
- [3] P. Koppenburg *et al.* [Belle Collaboration], Phys. Rev. Lett. **93**, 061803 (2004).
- [4] B. Aubert *et al.* [BaBar Collaboration], Phys. Rev. Lett. **97**, 171803 (2006).
- [5] E. Barberio *et al.* [Heavy Flavor Averaging Group], 0704.3575 [hep-ex] and online update available at <http://www.slac.stanford.edu/xorg/hfag/>.
- [6] B. Aubert *et al.* [BaBar Collaboration], 0711.4889 [hep-ex].
- [7] K. Bieri, C. Greub and M. Steinhauser, Phys. Rev. D **67**, 114019 (2003); M. Misiak and M. Steinhauser, Nucl. Phys. B **683**, 277 (2004); M. Gorbahn and U. Haisch, Nucl. Phys. B **713**, 291 (2005); M. Gorbahn, U. Haisch and M. Misiak, Phys. Rev. Lett. **95**, 102004 (2005); K. Melnikov and A. Mitov, Phys. Lett. B **620**, 69 (2005); I. Blokland *et al.*, Phys. Rev. D **72**, 033014 (2005); H. M. Asatrian *et al.*, Nucl. Phys. B **749**, 325 (2006) and **762**, 212 (2007).
- [8] M. Misiak and M. Steinhauser, Nucl. Phys. B **764**, 62 (2007).
- [9] M. Czakon, U. Haisch and M. Misiak, JHEP **03**, 008 (2007).
- [10] M. Misiak *et al.*, Phys. Rev. Lett. **98**, 022002 (2007).
- [11] H. M. Asatrian *et al.*, Phys. Lett. B **647**, 173 (2007).
- [12] R. Boughezal, M. Czakon and T. Schutzmeier, JHEP **0709**, 072 (2007).
- [13] K. Agashe, N. G. Deshpande and G. H. Wu, Phys. Lett. B **514**, 309 (2001).
- [14] A. J. Buras *et al.*, Nucl. Phys. B **678**, 455 (2004).
- [15] U. Haisch and A. Weiler, Phys. Rev. D **76**, 034014 (2007).
- [16] T. Appelquist, H. C. Cheng and B. A. Dobrescu, Phys. Rev. D **64**, 035002 (2001).
- [17] I. Gogoladze and C. Macesanu, Phys. Rev. D **74**, 093012 (2006).
- [18] G. Burdman, B. A. Dobrescu and E. Ponton, JHEP **0602**, 033 (2006).
- [19] G. Burdman, B. A. Dobrescu and E. Ponton, Phys. Rev. D **74**, 075008 (2006).
- [20] B. A. Dobrescu and E. Ponton, JHEP **0403**, 071 (2004); M. Hashimoto and D. K. Hong, Phys. Rev. D **71**, 056004 (2005).
- [21] B. A. Dobrescu *et al.*, JCAP **0710**, 012 (2007).
- [22] E. Ponton and L. Wang, JHEP **0611**, 018 (2006).
- [23] H. Georgi, A. K. Grant and G. Hailu, Phys. Lett. B **506**, 207 (2001).
- [24] H. C. Cheng, K. T. Matchev and M. Schmaltz, Phys. Rev. D **66**, 036005 (2002).
- [25] A. J. Buras, M. Spranger and A. Weiler, Nucl. Phys. B **660**, 225 (2003).
- [26] B. A. Dobrescu, K. Kong and R. Mahbubani, JHEP **0707**, 006 (2007).
- [27] B. A. Dobrescu, K. Kong and R. Mahbubani, 0709.2378 [hep-ph].
- [28] A. Freitas and K. Kong, 0711.4124 [hep-ph].
- [29] K. G. Chetyrkin, M. Misiak and M. Münz, Phys. Lett. B **400**, 206 (1997) [Erratum-ibid. B **425**, 414 (1998)].
- [30] P. Gambino and U. Haisch, JHEP **0009**, 001 (2000) and **0110**, 020 (2001).
- [31] A. J. Buras *et al.*, Nucl. Phys. B **424**, 374 (1994).
- [32] T. Hahn, Comput. Phys. Commun. **140**, 418 (2001).
- [33] S. L. Glashow, J. Iliopoulos and L. Maiani, Phys. Rev. D **2**, 1285 (1970).
- [34] R. S. Chivukula *et al.*, Phys. Lett. B **562**, 109 (2003).
- [35] P. Gambino, U. Haisch and M. Misiak, Phys. Rev. Lett. **94**, 061803 (2005); C. Bobeth *et al.*, Nucl. Phys. B **726**, 252 (2005); U. Haisch and A. Weiler, Phys. Rev. D **76**, 074027 (2007).
- [36] M. Misiak and M. Steinhauser, private communications (2007).